Supporting Information

Mechanism Investigation of the Post Necking Treatment to WO_3 Photoelectrodes

*Dapeng Cao,[a,b] Jie Wang,[a] Jingbo Zhang,[a] Shuaishuai Liu,[a] Futing Xu,[a] Song Xu,[a] Xin Xu,[a] Baoxiu Mi, *[a] Zhiqiang Gao*[b]*

[a] Key Laboratory for Organic Electronics & Information Displays (KLOEID), Jiangsu Engineering Centre for Plate Displays & Solid State Lighting, and Institute of Advanced Materials (IAM), Nanjing University of Posts & Telecommunications, Nanjing 210023, China

[b] Key Laboratory of Flexible Electronics, Jiangsu National Synergetic Innovation Center for Advanced Materials (SICAM), School of Material Science and Engineering, Nanjing University of Posts & Telecommunications, Nanjing, Jiangsu 210023, China.

Corresponding Author

*E-mail: iambxmi@njupt.edu.cn; iamzqgao@njupt.edu.cn.

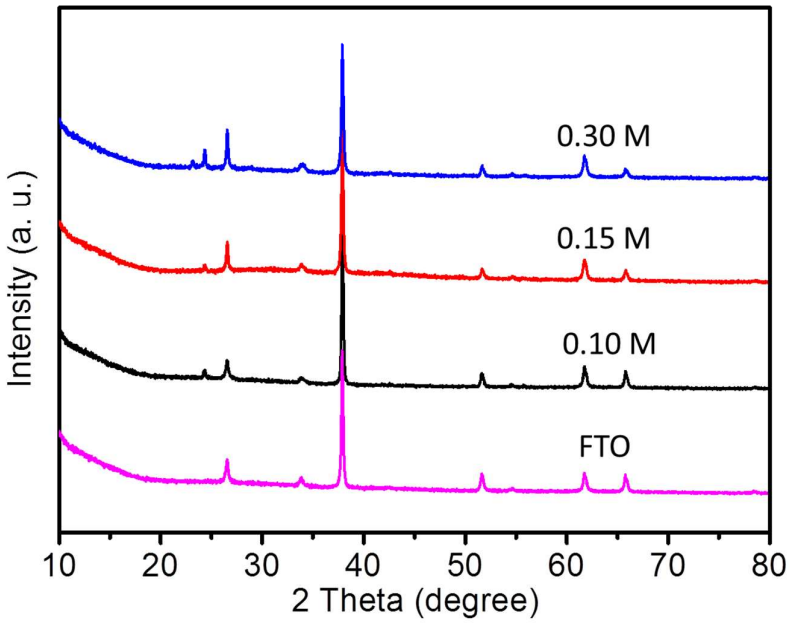

Figure S1. The XRD pattern of compact WO_3 films on FTO prepared from different concentration of ammonium metatungstate. The diffraction pattern of a bare FTO is shown for comparison.

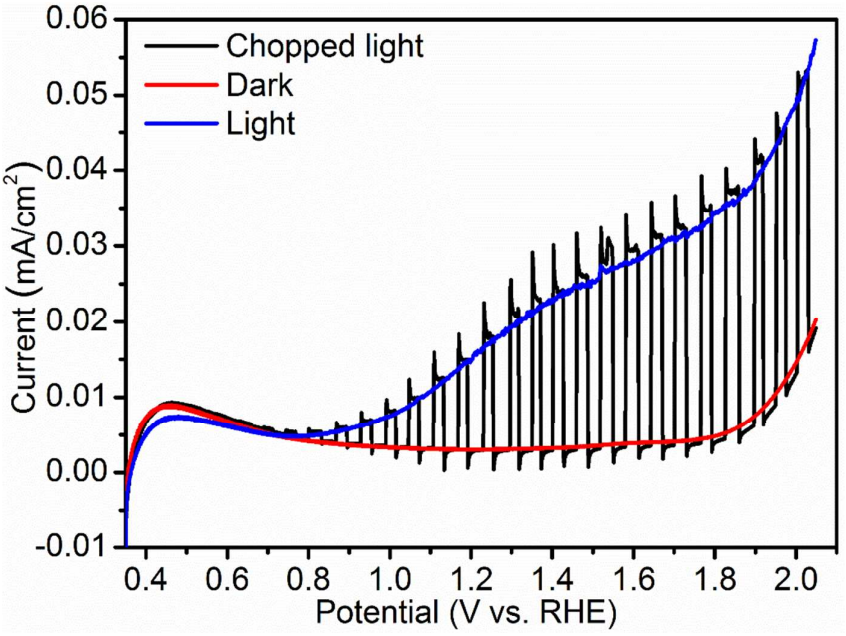

Figure S2. The current-potential curve of a WO_3 photoanode prepared by drop ammonium metatungstate followed by annealing.

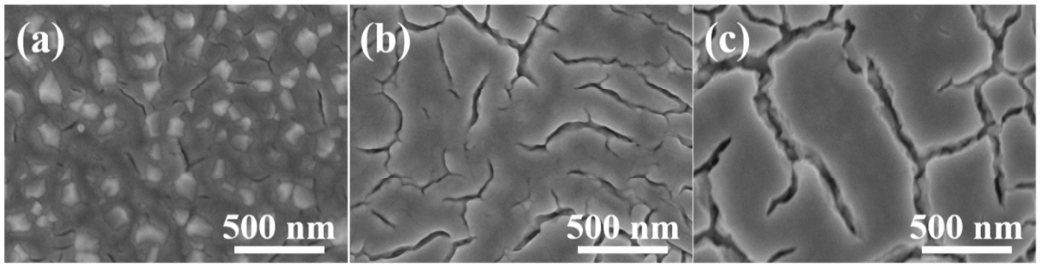

Figure S3. SEM images of the compact WO_3 layers prepared by spin-coating ammonium metatungstate solution on FTO followed by annealing at 450 ºC in air. The concentration of ammonium metatungstate solution is 0.1 M (a), 0.15 M (b) and 0.3 M (c).

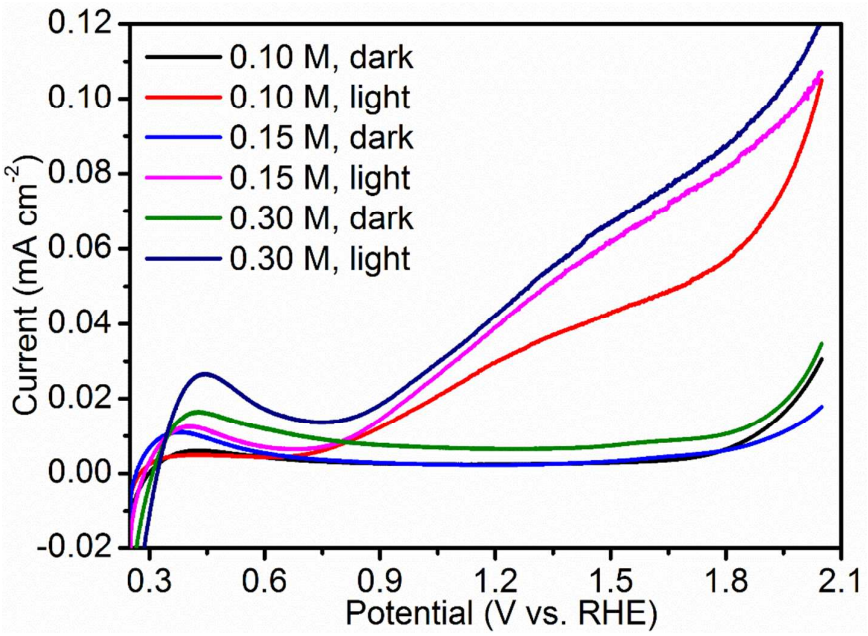

Figure S4. The current-potential curves of WO_3 photoanodes prepared by spin-coating ammonium metatungstate solution on FTO followed by annealing at 450 ºC in air.

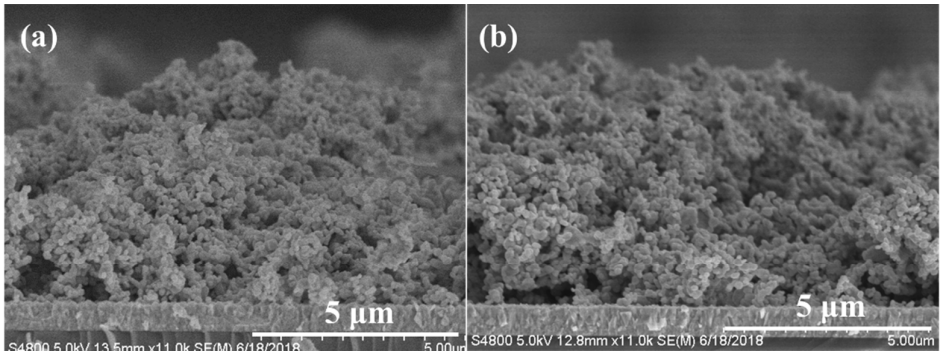

Figure S5. Section SEM images of the WO_3 films without (a) and with (b) a compact WO_3 layer.

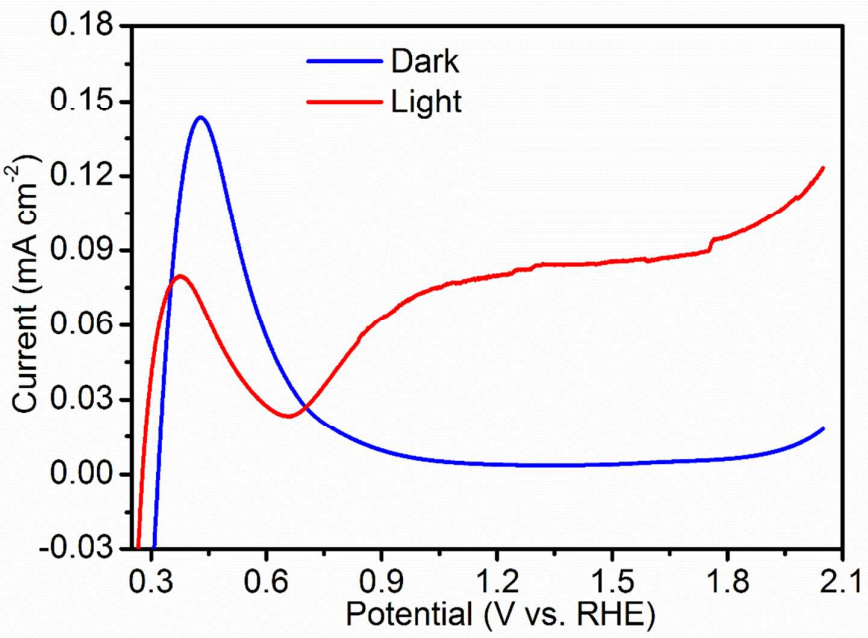

Figure S6. Current-potential curves of an as-deposited WO_3 photoanode with compact layer.

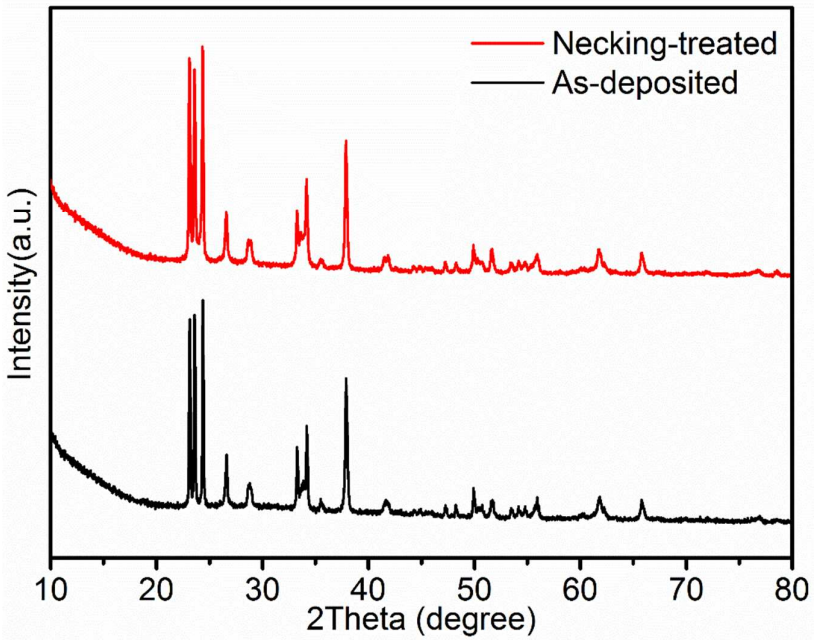

Figure S7. XRD pattern of as-deposited and necking-treated WO_3 films.

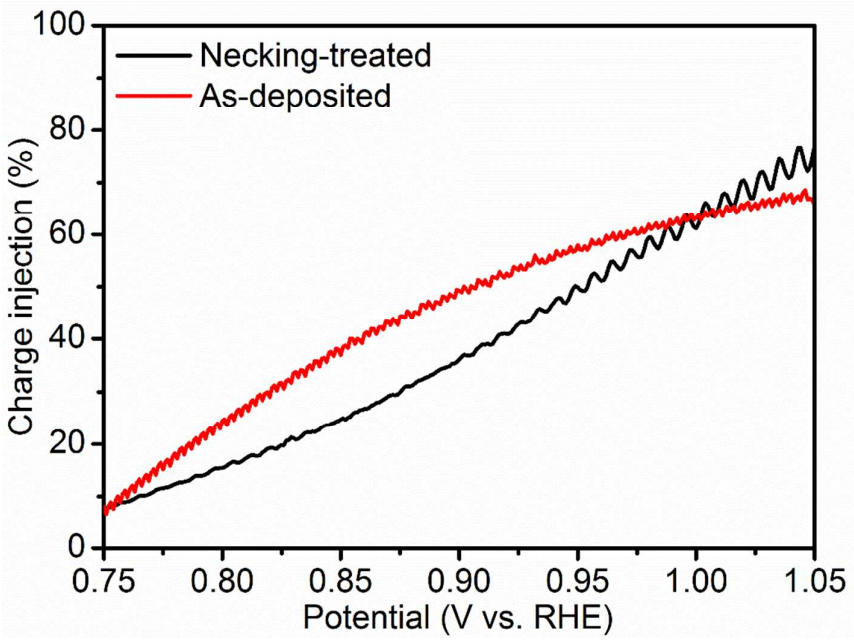

Figure S8. Yield of charge injection in the as-deposited WO_3 photoanode and the necking-treated WO_3 photoanode.

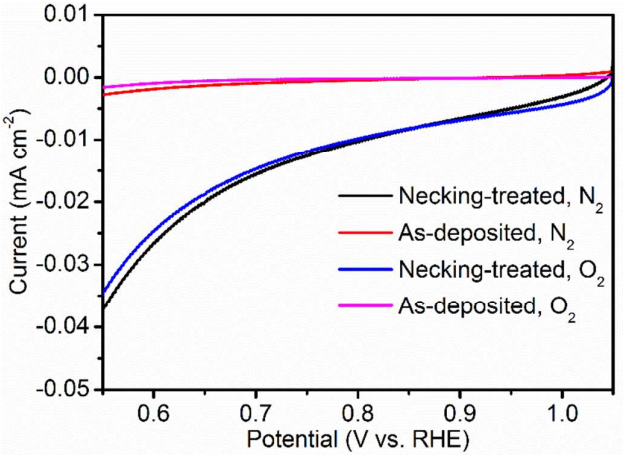

Figure S9. Reduction dark current on the as-deposited and necking-treated samples, electrolyte: 0.5 M Na_2SO_4 with N_2 or O_2 bubbling.

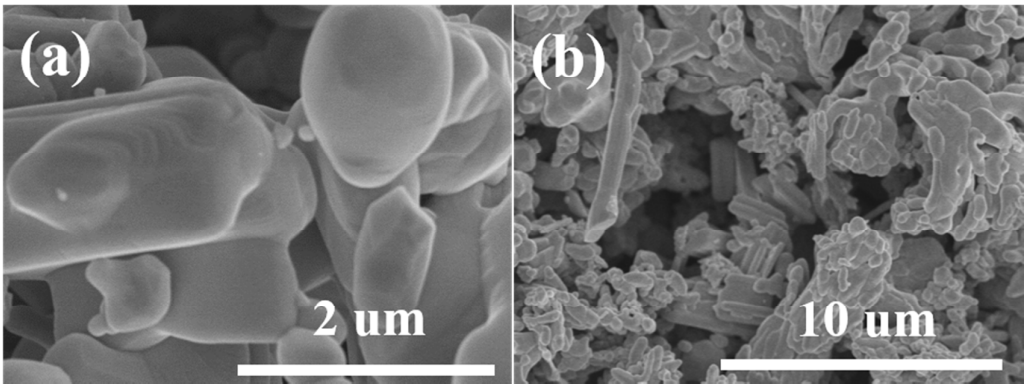

Figure S10. SEM images of a WO_3 photoanode prepared from large WO_3 particles at high (a) and low (b) magnification.

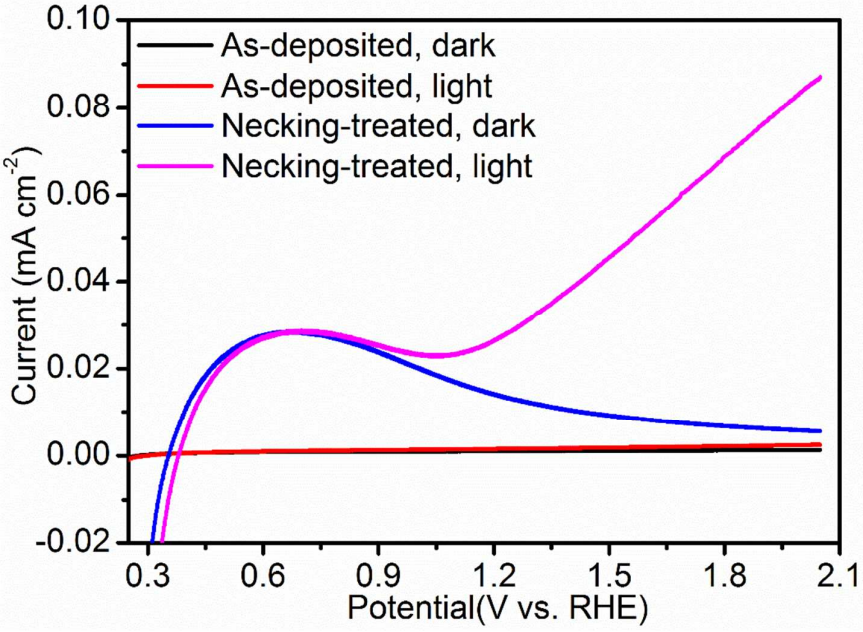

Figure S11. Current–potential curves of the WO_3 photoanodes (prepared from large WO_3 particles) without and with post necking treatment.

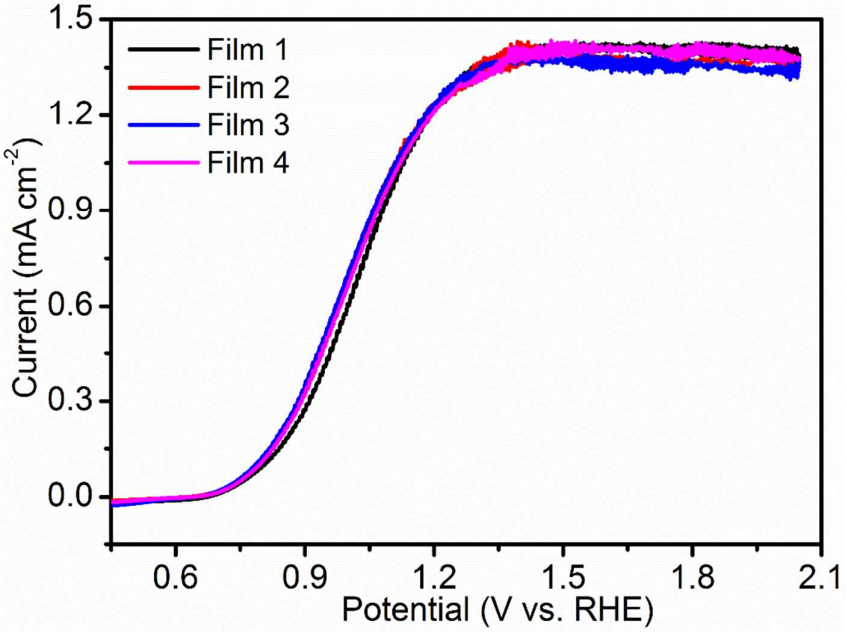

Figure S12. Current–potential curves of the necking-treated WO_3 photoanode with underlayer in 0.5 M Na_2SO_4 aqueous solution.

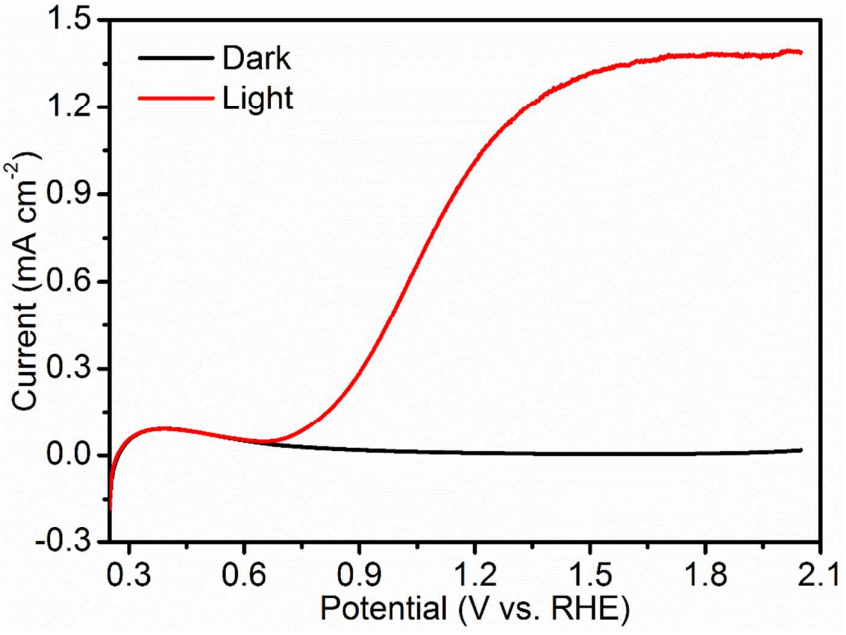

Figure S13. Current–potential curves of the necking-treated WO_3 photoanode after *I-t* test.

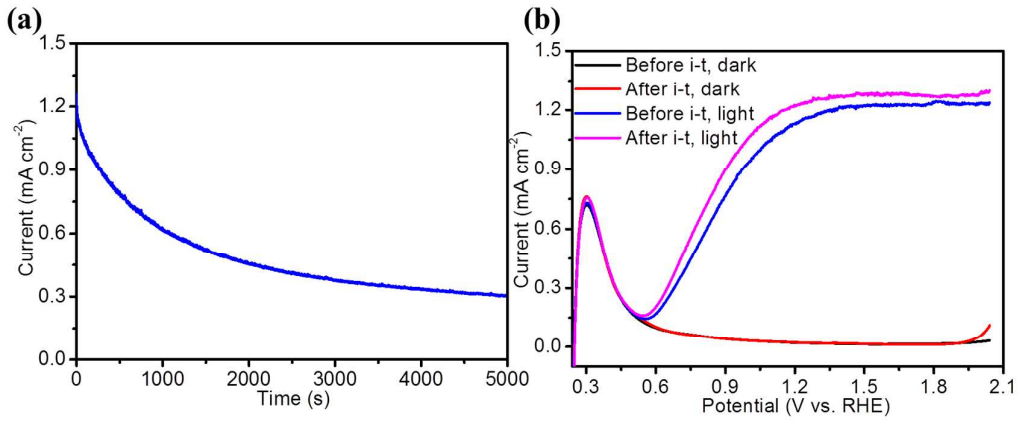

Figure S14. (a) *I-t* curves of the necking-treated WO_3 photoanode with underlayer at a potential of 1.65 V_{RHE}, (b) *I-V* curves of the necking-treated WO_3 photoanode with underlayer before and after the *I-t* test, electrolyte: 0.5 M H_2SO_4.